



# Numerical Study of H-Darrieus Turbine as a Rotor for Gravitational Vortex Turbine

Jorge Andrés Sierra Del Rio<sup>1,\*</sup>, Alejandro Ruiz Sánchez<sup>2</sup>, Daniel Sanín-Villa<sup>3</sup>, Edwin Correa Quintana<sup>2</sup>

<sup>1</sup> Department of Engineering, Environmental Research Group – GIIAM, Institución Universitaria Pascual Bravo, Medellín, Colombia

<sup>2</sup> Department of Mechatronics Engineering, Research Group – MATyER, Instituto Tecnológico Metropolitano, Medellín, Colombia

<sup>3</sup> Department of Engineering, Investigación e Innovación en energía Group – GIEN, Institución Universitaria Pascual Bravo, Medellín, Colombia

## ARTICLE INFO

### Article history:

Received 5 May 2022

Received in revised form 4 July 2022

Accepted 19 July 2022

Available online 31 August 2022

### Keywords:

Vortex; geometry; turbine; energy;

Darrieus; CFD; rotor

## ABSTRACT

The main objective of this study is to compare numerically the torque generated at 50, 75, 100, and 125 rpm by H-Darrieus turbine as a rotor for Gravitational Vortex Turbine. The rotational flow into the gravitational vortex turbine tank helped to decrease the negative torque in H-Darrieus rotor. The study was developed in ANSYS® CFX, where the model was configured at constant operating conditions. The highest torque was 0.117 Nm at 50 rpm, and the torque decreased with increasing rpm. The H-Darrieus works with increasing lift force, however, the rotor inside the Gravitational Vortex Turbine interacts with drag force.

## 1. Introduction

The gravitational vortex turbine (GVT) is an alternative to renewable energies. It is a small-scale turbine that converts the fluid's kinetic energy by forming vortex into electrical power through a generator [1]. Figure 1 exemplifies the operation and parts of the turbine (designated as standard tank). The tank geometry is configured in the direction of flow through an open channel of rectangular section, which leads to and stabilizes the flow of water that has been derived from the river. Then through an eccentric reduction, while maintaining the height of the channel, the flow is accelerated fluid before entering the upper part of the tank, which is generally configured as a cylindrical tank with a circular and concentric outlet located at the bottom concerning the level of the inlet channel [2]. The fluid enters horizontally and tangentially, but due to the circular geometry of the tank and the difference in level between the entrance and exit of the chamber, a rotation of the fluid is induced with respect to the exit orifice known as a gravitational vortex, which is form due to the joint action of the gravitational force and the Coriolis force [3]. For a streamline, the path that the water takes inside the chamber tank can be represented by a spiral that rotates around the axis

\* Corresponding author.

E-mail address: [jorgesierra@itm.edu.co](mailto:jorgesierra@itm.edu.co) (Jorge Andrés Sierra Del Rio)

of the air core, which is formed by conservation of momentum between two fluids, water, and air in this case.

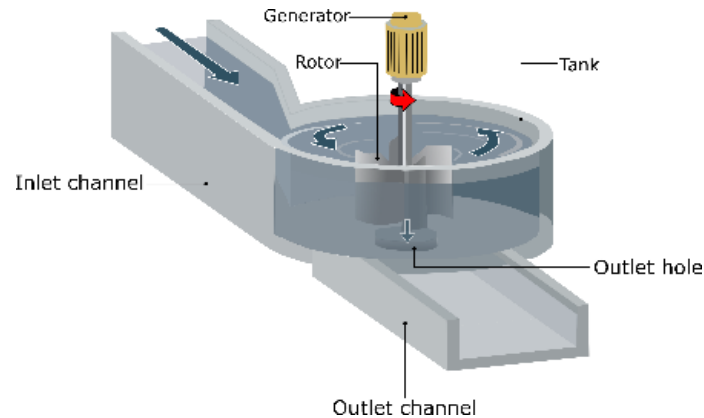


**Fig. 1.** GVT parts, Adapted from ref. [4]

Table 1 shows the installed GVTs that have been found to date in the world. Europe has nine installed, followed by Asia with three, South America with two and Oceania with one. The power generated by each turbine depends on its use (domestic or machinery). For this reason, the Swiss turbine stands out for being the most significant power generator at a lower flow rate and height. To exemplify Table 1 the calculation of the electrical power of Eq. (1) [1] was taken.

$$P_{\text{electrical}} = Q \cdot \rho \cdot h \cdot g \cdot \eta_t \quad (1)$$

Where  $\eta_t$  is the efficiency of the GVT (where the generator has an efficiency of 90%). However, the turbine efficiency calculations are not concise in the literature, and in some cases, it is not mentioned [5].

**Table 1**  
 GVT installed worldwide

Country	City	Year	Heigh (m)	Flow (m <sup>3</sup> /s)	Power (kW)
Swiss [6]	Schöftland	2009	1,5	1	15
Indonesia [7]	Bali	2015	1,8	1	15
Chile [8]	Doñihue	2017	2,1	2	15
Australia [9]	Marysville	2013	0,6	0,11	11
Italy [10]	Sureste Sesto Campano	2017	1,5	1	9
Italy [10]	Noreste Bivio Mortola	2017	1,8	0,8	9
Thailand [10]	Oeste Taksinmaharat	2014	1,5	1	8,5
Austria [1]	Obergrafendorf	2005	0,9	0,9	8,3
Peru [10]	Junin	2016	1,4	0,9	7,2
Germany [10]	Wesentz, Sachsen	2013	1,2	0,5	6
Germany [10]	Niedersfel, Winterberg	2012	1,4	0,5	4,7
Lithuania [10]	Este Kaunas	2010	1,5	0,5	4,4
Italy [10]	Suroeste San Vito	2014	0,4	0,9	4
Austria [10]	Norte St. Veit an der Glan	2011	0,9	0,7	3,3
Nepal [11]	Katmandú	2016	1,5	0,2	1,6

Wanchat *et al.*, [12] through a numerical study in Ansys Fluent determined the incidence of the height of the water level and the geometry of the tank in the tangential velocity of the generated vortex. The study concludes that the tangential velocity is directly proportional to the height of the

water level inside the tank. Furthermore, the authors find that the (standard) circular tank exhibits a symmetric vortex formation.

Gheorghe *et al.*, [13] presented a numerical study in which the radial, axial and tangential velocity was analyzed in a GVT with a conical tank, and a rotor made up of three types of blades located at three different heights of the tank and with different diameters. The authors found that the radial and axial velocities reach the maximum value between the vortex surface and the sidewall of the conical tank because, at the limits of the wall, these velocities are zero. On the other hand, the tangential velocity increases as it moves away from the tank walls, reaching maximum values near the core of the vortex and at the bottom of the tank.

Daka *et al.*, [14] determined through a numerical study the effect of the geometry of a chamber with a conical tank on the power generated. According to the authors, a tank with a diameter of 0.52 m, a conicity of the tank of 23°, an inlet width of the reduced area to the tank of 0.1 m, a height of the water inside the tank of 0.4 m, and an angle of channel reduction of 43° represent the best geometry for the operating conditions established in the study.

Wanchat *et al.*, [15] determined the relationship between the outlet hole diameter and the electrical power of the standard tank GVT. For the development of the study, a rotor made up of 5 blades was implemented, an input speed of 0.1 m/s was established, and variations were made in the output diameter of the GVT from 0.1m to 0.4. The study concluded that the diameter range for the outlet orifice is between 14% and 18% of the tank diameter.

Mulligan *et al.*, [17] presented an analytical, numerical, and experimental study of vortex formation in a cylindrical tank to establish the turbulence model that best represents the geometry of the vortex and the tangential velocity inside it. The authors found that the model best representing the experimental results corresponds to the BSL RSM turbulence model. Once the BSL RSM turbulence model has been selected, the vortex formation for three different inlet flows is compared with the analytical study proposed by Vatista in [16] and the experimental study. It is concluded that the analytical model proposed by Vatista showed significant similarity with the experimental and numerical analysis [17].

Shabara *et al.*, [18] performed a numerical study in Ansys Fluent with experimental validation. The geometry implemented for the GVT was the one proposed by Franz Zotlöterer. Errors of 2% and 7% between the numerical and experimental results determined the validity of the numerical model. It is concluded that the water inlet height in the turbine is not a parameter that significantly influences the efficiency of the GVT compared to the incidence of the tank's geometry.

Dakal *et al.*, [19] carried out the experimental validation of a numerical analysis carried out in Ansys Fluent, in which the efficiency of two GVTs with different tank geometries is compared: conical and cylindrical, both models under the same operating conditions (inlet speed, pressure, etc.). The numerical and experimental results showed that the conical tank turbine obtained better performance than the cylindrical one by comparing the outlet velocities values. In the experimental study, the conical tank presented a higher efficiency than the cylindrical tank measured to the electrical power generated by the same generator, presenting efficiency values of 36.8% and 20.9%, respectively.

As evidenced in the state of the art, studies around GVT have focused on tank design and analytical studies. However, few investigations have studied the rotor, this being a parameter that highly influences the efficiency of the GVT. The objective of the present study is to numerically evaluate an H-Darrieus turbine as a rotor of a gravitational vortex turbine.

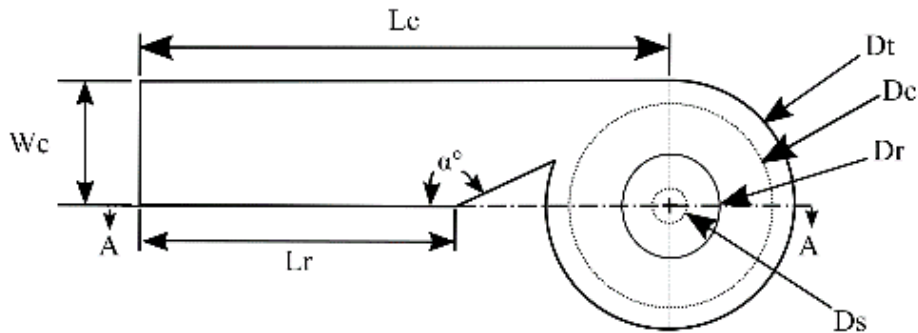
## 2. Methodology

In the present study, GVT was performed with an exit hole ratio of 14% as suggested by Wanchat *et al.*, [20], and the Darrieus rotor. This rotor will be studied because there is little research on the design of the rotor of a gravitational vortex turbine which is one of the main parameters affecting the efficiency of hydraulic turbines [21]. In addition to this, one of the main problems of the H-Darrieus turbine that affects its performance is the counter-torque generated in the blades [22] and due to the rotational flow of the GVT, this can be reduced, increasing the performance of the turbine.

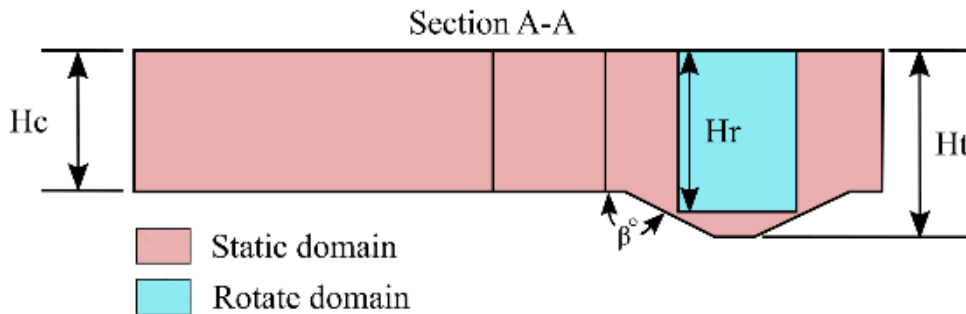
The appropriate dimensions were selected for the tank design parameters, such as: conicity angle and notch angle [14]. Table 2 shows the sizes used for each parameter of the GVT studied. Figure 2.a shows the sketch of the GVT and its respective dimensions, and Figure 2.b graphically represents the dimensions between the static and rotational domains.

**Table 2**  
 GVT dimensión

Parameter	Value
Tank diameter (Dt)	0.70 m
Cone diameter (Dc)	0.57 m
Outlet hole diameter (Ds)	0.09 m
Rotor diameter (Dr)	0.35 m
Notch angle ( $\alpha$ )	155°
Length inlet channel (Lc)	1.50 m
Length area reduction (Lr)	0.90 m
Chanel width (Wc)	0.35 m
Chanel height (Hc)	0.35m
Tank height (Ht)	0.45 m
Rotate domain height (Hr)	0.35 m
Cone angle ( $\beta$ )	157°



(a) GVT dimensions



(b) Static and rotate domain

**Fig. 2.** GVT sketch

After generating the GVT camera, a concentric emptying was created in the upper part of the tank with a diameter of 0.35 m and a depth of 0.35 m, in which the rotor of the study was entered and evaluated. These dimensions are taken from the study by Dhakal *et al.*, [19] that mentions that the conical turbine presents a higher percentage of speed and a higher tangential velocity in the interaction between the fluid and the air vortex. Figure 3 represents the cast generated in the CAD of the GVT. The modeling of the rotor will start from the same principle that was started for the camera. Once the design parameters were selected, we proceeded with the sketch and then with the extrusion. Table 3 represents which parameters were considered for the elaboration of the rotor. According to Kumar *et al.*, [22] the predominant driving force for a Darrieus rotor is the lift force. The NACA 2408 profile was selected, which has a maximum lift over drag ratio ( $C_l/C_d$ ) of 37.4 [21]. The main objective of H-Darrieus turbine is decrease the negative torque of the incoming blade [22-24] in GVT case, the flow is rotational inside the chamber.

**Table 3**  
Rotor dimentions

Parameter	Value
Diameter	0.35 m
Height	0.13 m
Blades	3

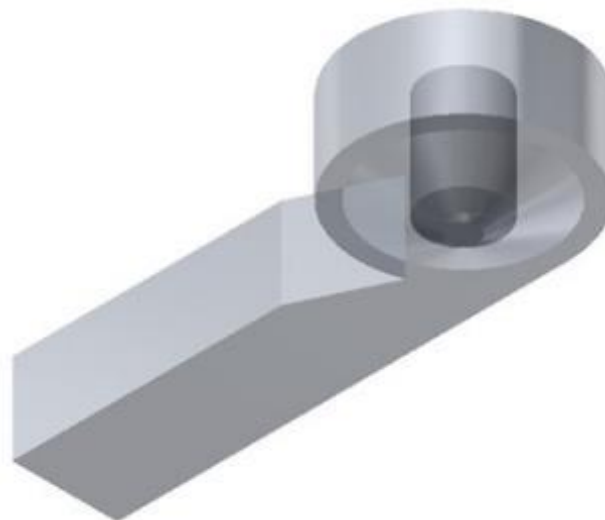


**Fig. 3.** Camera and rotor assemble

The discretization of volume control was carried out in Ansys ICEM<sup>®</sup> modules for having higher quality metrics in the meshes [25], supervising as a significant dimension the minimum orthogonal quality, which varies between zero and one, being one the value is associated with the best quality of the mesh [26-28] the aspect ratio and the minimum determinant 3x3. For the camera and rotor, 34 blocks were made, 18 and 16, respectively. In this way, it is guaranteed that all the elements are hexahedral. Figure 4 represents the blocks created for the chamber, these blocks were made with greater emphasis on area reduction and the conical discharge section. The thickness of the first boundary layer is 0.038 mm, with a  $Y^+$  of 90.

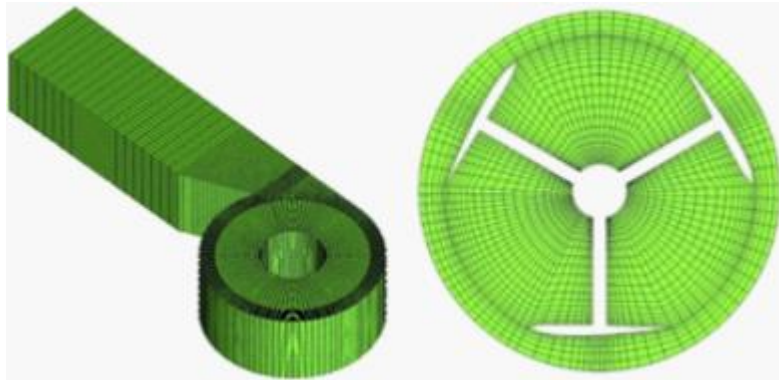


Fig. 4. Camera and rotor mesh

The simulation was performed in a transitory state, with a total time of 15s and a time step of 1ms, guaranteeing a Courant number less than 1 [29, 30] guaranteeing that only one element is not evaluated in each step time. A convergence criterion of 1E-4 was selected to ensure reliable results [27]. The turbulence model chosen was the Baseline Reynold Stress Model for having reliable results in rotational fluids [31]. Figure 5 represents the boundary conditions in the GVT, and Table 4 describethe values established for each condition.

**Table 4**  
 Boundary conditions values for GVT

Condition	Type	Value
Inlet	Normal velocity	0.2 m/s
Outlet	Open pressure	0 Pa
Wall	Slider	-
Opening	Open pressure	0 Pa
State	Transitory	$\Delta t = 0.001$ s
Interface	Transient rotor stator	-
Angular velocity	rotor	[50, 75, 100, 125] rpm

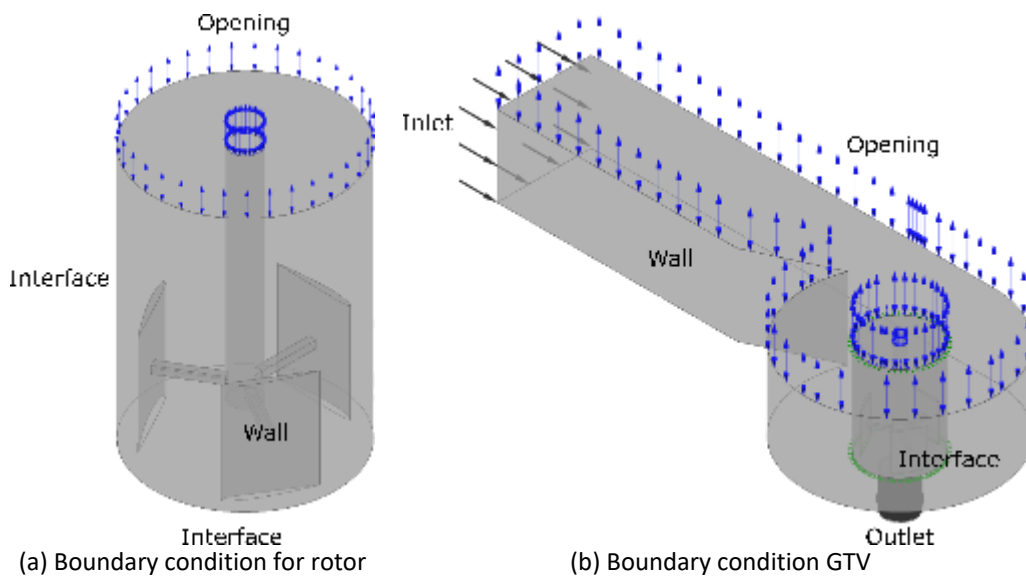


Fig. 5. Boundary condition

### 3. Results

#### 3.1 Mesh Study

Figure 6 represents the mesh independence for GVT corresponding to the study. The simulations were performed approximately up to 1.1E6 elements where the results do not vary significantly (less than 5% difference) [26, 27, 32, 33] with an angular speed of 50 rpm for the rotor; therefore, a mesh of approximately 3.9E5 elements was selected to follow the simulations.

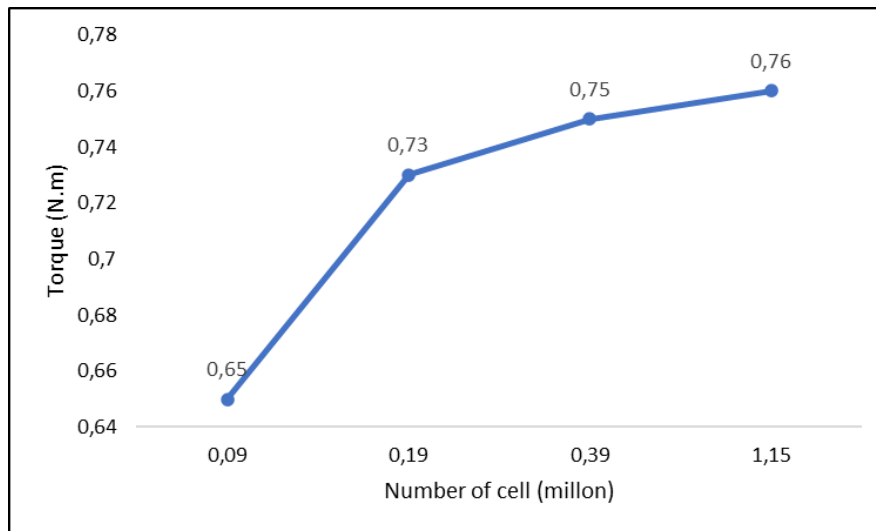


Fig. 6. Mesh study in GVT

#### 3.1.1 The effect of angular velocity

Once the GVT mesh had been selected, the angular speed of the rotor varied from 50 rpm to 125 rpm to obtain the behavior of the torque at different angular velocities. Figure 7 shows how the torque varies according to the increase in rpm, being 50 rpm the one with the highest torque, generating 0.117 Nm, and 120 rpm the one with the low torque, causing 0.084 Nm. The difference between 50 and 75 rpm is 1.7%, which does not represent a significant difference between both. However, the largest difference is 28% and is presented to 125 rpm as rotor angular velocity.

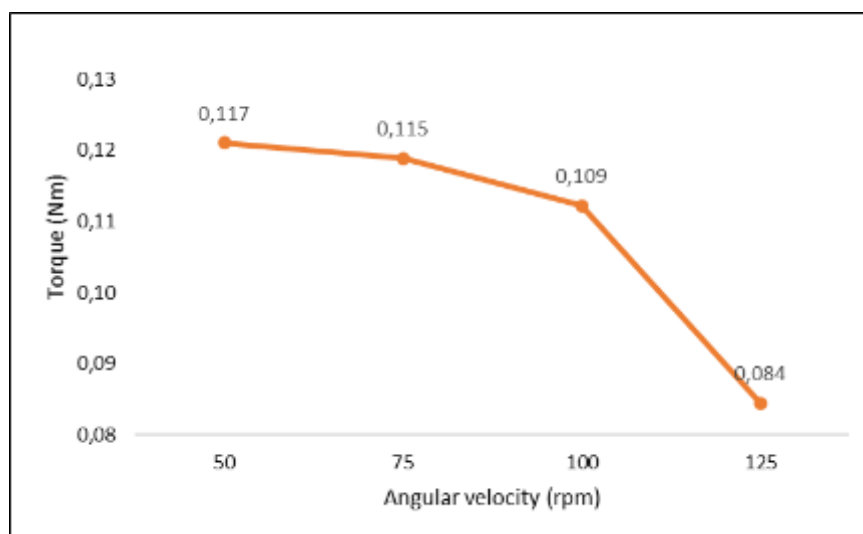


Fig. 7. Generated torque vs angular velocity in GVT

Figure 8 shows the streamlines in the GVT tank and how they interact with the rotor. It should be noted that when the fluid enters the tank, it already enters stabilized thanks to the inlet channel and with a pre-rotation induced by the notch angle to reduce turbulence in the tank. Furthermore, the streamlines also exemplify the behavior of the fluid when it hits the rotor in the center of the tank, where the vortex deforms completely. However, the core formed in the tank does not interact with much of the rotor blade surface area due to its size. As mentioned above, in the H-Darrieus turbine the lift force predominates [34], therefore the blade design does not have a large surface area to interact with the GVT fluid.

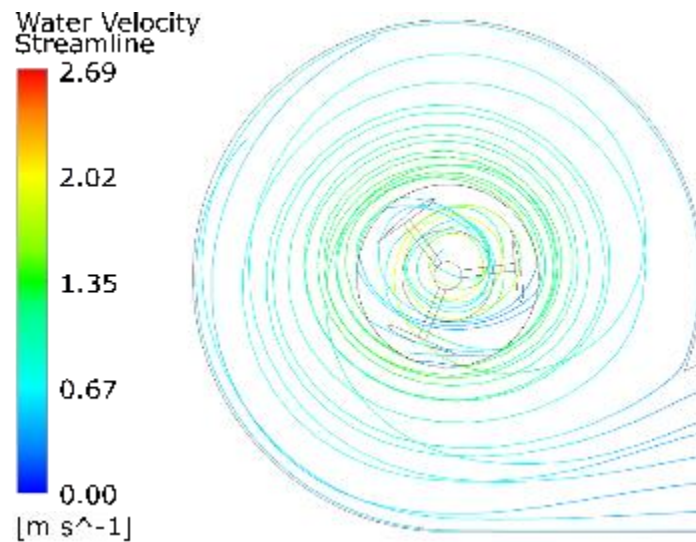


Fig. 8. Water velocity streamlines

Figure 9 shows the pressure contour in different parts of the rotor. In these results, the highest pressure in each blade is at its lower tip, corroborating the behavior of the fluid in the vortex, where the velocity increases as it descends and approaches the center of the tank. In addition to what has been said above, it can also be seen that the inner face (pointing towards the rotor axis) of the blades does not interact directly with the fluid, contrary to the outer face, which is where the fluid impacts once it approaches the center of the tank. Table 5 describes the values of the pressure points in kPa, referencing the point P1 that corresponds to the lower corner of the blade facing the fluid when it enters the tank. With regard to the above, by presenting the maximum point of fluid pressure in the lower part, it does not take advantage of much of the kinetic energy of the fluid in the chamber. The difference between point P1 and P1.1 (Only the height between points changes) is 22% in pressure can be observed, demonstrating that H-Darrieus turbine as a GVT rotor does not take great advantage of the behavior of the fluid inside tank. Thanks to this, it can also be seen that point P2 is the one with the greatest pressure difference (47%) with respect to point P1, where this point P2 does not present significant pressure to rotate the rotor.

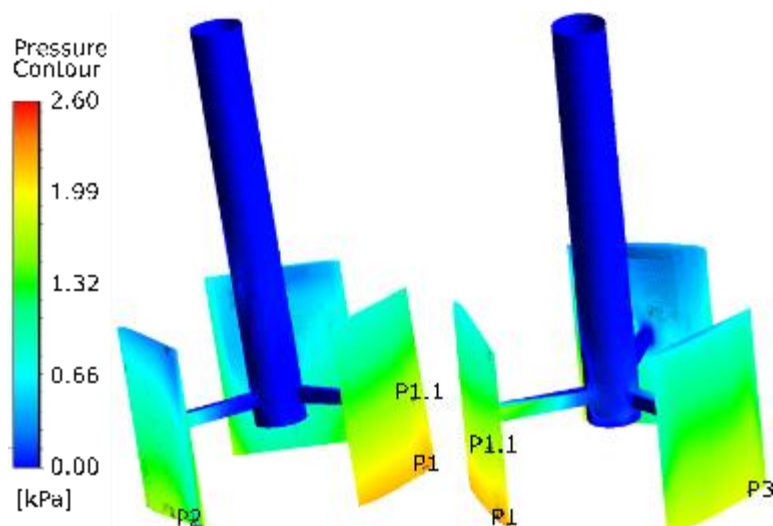


Fig. 9. Pressure contour generated by water in blades

**Table 5**  
 Local max pressure in blade faces

Point	Location (m)			Pressure (KPa)	Difference (%)
	X	Y	Z		
P1	0.052	-0.152	0.087	2.18	0
P1.1	0.052	-0.100	0.087	1.68	22
P2	0.055	-0.152	-0.087	1.15	47
P3	-0.102	-0.152	-0.001	1.84	15

According to the results, the H-Darrieus rotor works with increasing lift force [22, 35]. However, the rotor inside the GVT interacts with drag and not lift force [36], which does not allow a better performance of this rotor. It must be considered that the area of the blade face perpendicular to the fluid is less than that of the conventional rotor (straight blades); therefore, this also directly influences the performance of the GVT given that the greater the contact area of the fluid with the rotor, the drag force on the rotor increases.

#### 4. Conclusions

The GVT is positioned as one of the alternatives in the generation and consumption of energy near it, thanks to its easy manufacturing and low maintenance that it requires. One of the main parameters that affect the performance of the GVT is the rotor; however, most of the studies focus on the design of the tank and the formation of the vortex. The present study proposed a three blades H-Darrieus rotor for the GVT where it presented a significant difference in the water pressure in the blades with differences of up to 47%, corroborating that the fluid increases its speed as it approaches the center and the tank bottom. Also, it was found that the range between 50 and 75 rpm as angular velocity of the rotor presents higher performance and does not present a significant difference (less than 2%), contrary to 100 rpm or more where the difference begins to increase up to 28%. Thanks to this, it is determined that the design of the rotor in a gravitational vortex turbine greatly influences its performance.

Continuing with the previous idea, the entire research community can be invited to study a chamber-rotor configuration for the gravitational vortex turbine in order to increase the performance of this turbine considerably. Among the rotor designs that can be studied is the Savonius and a truncated rotor, keeping in mind that the selected rotors must work with the drag force principle.

## Acknowledgement

The authors are grateful to Instituto Tecnológico Metropolitano's Models Laboratory and MATyER research group in Medellín, Colombia, for giving the opportunity to develop the numerical study of the present research.

## References

- [1] F. Zotlöterer, "Gravitational Water Vortex Power Plants," 2003. <http://www.zotloeterer.com/welcome/gravitation-water-vortex-power-plants/configuration-function/> (accessed Mar. 04, 2018).
- [2] Sierra, Jorge, Alejandro Ruiz, Angie Guevara, and Alejandro Posada. "Gravitational Vortex Turbines as a Renewable Energy." *International Journal of Fluid Machinery and Systems* 13, no. 4 (2020): 704-717. <https://doi.org/10.5293/IJFMS.2020.13.4.704>
- [3] Li, Hai-feng, Hong-xun Chen, Zheng Ma, and Yi Zhou. "Formation and influencing factors of free surface vortex in a barrel with a central orifice at bottom." *Journal of hydrodynamics* 21, no. 2 (2009): 238-244. [https://doi.org/10.1016/S1001-6058\(08\)60141-9](https://doi.org/10.1016/S1001-6058(08)60141-9)
- [4] B. Petrovic, "Micro Usina Hidreléctrica Baseada no Vórtice Gravitacional," Intituto Nikola Tesla.
- [5] Sánchez, Alejandro Ruiz, Jorge Andrés Sierra Del Rio, Angie Judith Guevara Muñoz, and José Alejandro Posada Montoya. "Numerical and experimental evaluation of concave and convex designs for gravitational water vortex turbine." *Journal of Advanced Research in Fluid Mechanics and Thermal Sciences* 64, no. 1 (2019): 160-172.
- [6] Wasserwirbe, "Genossenschaft Wasserwirbel Konzepte Schweiz," 2017. <http://gwwk.ch/> (accessed Mar. 05, 2018).
- [7] Green by Jonh;, "Vortex at Green School," 2015. <http://greenbyjohn.com/vortex-at-green-school/> (accessed Apr. 11, 2018).
- [8] Turbulent;, "Turbulent micro hydropower," 2019. <http://www.turbulent.be/> (accessed Mar. 05, 2018).
- [9] KCT, "KOURIS CENTRI TURBINE," 2016. <http://www.kcthydropower.com/>.
- [10] Wasserwirbelkraftwerk, "Wasserwirbelkraftwerk," 2017. <http://wasserwirbelkraftwerk-de.simplesite.com/434308050>.
- [11] Dhakal, Rabin, A. Nepal, A. Acharya, B. Kumal, T. Aryal, S. J. Williamson, K. Khanal, and L. Devkota. "Technical and economic prospects for the site implementation of a gravitational water vortex power plant in Nepal." In *2016 IEEE International Conference on Renewable Energy Research and Applications (ICRERA)*, pp. 1001-1006. IEEE, 2016. <https://doi.org/10.1109/ICRERA.2016.7884485>
- [12] Wanchat, Sujate, and Ratchaphon Suntivarakorn. "Preliminary design of a vortex pool for electrical generation." *Advanced Science Letters* 13, no. 1 (2012): 173-177. <https://doi.org/10.1166/asl.2012.3855>
- [13] MARIAN, CB Gheorghe-Marius, Tudor SAJIN, Iulian FLORESCU, Dragos-Iulian NEDELICU, and Constantin-Narcis OSTAHIE. "the Concept and Theoretical Study of Micro Hydropower Plant With Gravitational the Concept and Theoretical Study of Micro Hydropower Plant With Wit H Gravitational Vortex and." In *World Energy Syst. Conf*, no. 3, pp. 219-226. 2012.
- [14] Dhakal, Sagar, Ashesh Babu Timilsina, Rabin Dhakal, Dinesh Fuyal, Tri Ratna Bajracharya, and Hari Prasad Pandit. "Effect of dominant parameters for conical basin: Gravitational water vortex power plant." In *Proceedings of IOE graduate conference*, vol. 5, p. 381. 2014.
- [15] Kueh, Tze Cheng, Shiao Lin Beh, Dirk Rilling, and Yongson Ooi. "Numerical analysis of water vortex formation for the water vortex power plant." *International Journal of Innovation, Management and Technology* 5, no. 2 (2014): 111.
- [16] Vatistas, G. H., S. Lin, and C. K. Kwok. "Theoretical and experimental studies on vortex chamber flows." *AIAA journal* 24, no. 4 (1986): 635-642. <https://doi.org/10.2514/3.9319>
- [17] Mulligan, S., J. Casserly, and R. Sherlock. "Experimental and numerical modelling of free-surface turbulent flows in full air-core water vortices,[In:] Gourbesville P., Cunge J., Caignaert G.(Eds) *Advances in Hydroinformatic*." (2014): 549-569. <https://doi.org/10.1007/978-981-287-615-7>
- [18] Shabara, H. M., O. B. Yaakob, Yasser M. Ahmed, A. H. Elbatran, and Muhammad SM Faddir. "CFD validation for efficient gravitational vortex pool system." *Jurnal Teknologi* 74, no. 5 (2015). <https://doi.org/10.11113/jt.v74.4648>
- [19] Dhakal, Sagar, Ashesh B. Timilsina, Rabin Dhakal, Dinesh Fuyal, Tri R. Bajracharya, Hari P. Pandit, Nagendra Amatya, and Amrit M. Nakarmi. "Comparison of cylindrical and conical basins with optimum position of runner: Gravitational water vortex power plant." *Renewable and Sustainable Energy Reviews* 48 (2015): 662-669. <https://doi.org/10.1016/j.rser.2015.04.030>
- [20] Wanchat, Sujate, Ratchaphon Suntivarakorn, Sujin Wanchat, Kitipong Tonmit, and Pongpun Kayanyiem. "A parametric study of a gravitation vortex power plant." In *Advanced Materials Research*, vol. 805, pp. 811-817. Trans Tech Publications Ltd, 2013. <https://doi.org/10.4028/www.scientific.net/AMR.805-806.811>

- [21] Kumar, Anuj, and Rajeshwer Prasad Saini. "Performance parameters of Savonius type hydrokinetic turbine—A Review." *Renewable and Sustainable Energy Reviews* 64 (2016): 289-310. <https://doi.org/10.1016/j.rser.2016.06.005>
- [22] Patel, Vimal, T. I. Eldho, and S. V. Prabhu. "Performance enhancement of a Darrieus hydrokinetic turbine with the blocking of a specific flow region for optimum use of hydropower." *Renewable Energy* 135 (2019): 1144-1156. <https://doi.org/10.1016/j.renene.2018.12.074>
- [23] Dabachi, Mohamed Amine, Abdellatif Rahmouni, and Otmame Bouksour. "Design and aerodynamic performance of new floating H-darrieus vertical Axis wind turbines." *Materials Today: Proceedings* 30 (2020): 899-904. <https://doi.org/10.1016/j.matpr.2020.04.347>
- [24] Dabachi, Mohamed Amine, Marwane Rouway, Abdellatif Rahmouni, Otmame Bouksour, Sara Jamoudi Sbai, Houda Laaouidi, Mostapha Tarfaoui, Abdelwahed Aamir, and Oumnia Lagdani. "Numerical Investigation of the Structural Behavior of an Innovative Offshore Floating Darrieus-Type Wind Turbines with Three-Stage Rotors." *Journal of Composites Science* 6, no. 6 (2022): 167. <https://doi.org/10.3390/jcs6060167>
- [25] Du, Jiyun, Zhicheng Shen, and Hongxing Yang. "Effects of different block designs on the performance of inline cross-flow turbines in urban water mains." *Applied energy* 228 (2018): 97-107. <https://doi.org/10.1016/j.apenergy.2018.06.079>
- [26] Ardila, Juan, Diego Hincapié, and Julio Casas. "Numerical models validation to correlations development for heat exchangers." *Actas Ing* 1 (2015): 164-168.
- [27] Ceballos, Y. Castañeda, M. Cardona Valencia, Diego Hincapie Zuluaga, J. S. Del Rio, and S. V. García. "Influence of the number of blades in the power generated by a Mitchell Banki Turbine." *International Journal Of Renewable Energy Research IJRES* 7, no. 4 (2017): 1989-1997.
- [28] Qing, Nelvin Kaw Chee, Nor Afzanizam Samiran, and Razlin Abd Rashid. "CFD Simulation analysis of Sub-Component in Municipal Solid Waste Gasification using Plasma Downdraft Technique." *Journal of Advanced Research in Numerical Heat Transfer* 8, no. 1 (2022): 36-43.
- [29] ANSYS, "Courant number," in ANSYS HELP, 2019.
- [30] Elfaghi, Abdulhafid MA, Alhadi A. Abosbaia, Munir FA Alkbir, and Abdoulhdi AB Omran. "CFD Simulation of Forced Convection Heat Transfer Enhancement in Pipe Using Al<sub>2</sub>O<sub>3</sub>/Water Nanofluid." *Journal of Advanced Research in Numerical Heat Transfer* 8, no. 1 (2022): 44-49.
- [31] Mulligan, S., J. Casserly, and R. Sherlock. "Experimental and numerical modelling of free-surface turbulent flows in full air-core water vortices,[In:] Gourbesville P., Cunge J., Caignaert G.(Eds) Advances in Hydroinformatic." (2014): 549-569.
- [32] Gómez, F. Hoyos, JD Betancur Gómez, D. Osorio Patiño, and JG Ardila Marín. "Construcción de curvas de factor de concentración de esfuerzos por medio de simulaciones." *Revista Cintex* 21, no. 1 (2016): 35-43.
- [33] Subramaniam, Thineshwaran, and Mohammad Rasidi Rasani. "Pulsatile CFD Numerical Simulation to investigate the effect of various degree and position of stenosis on carotid artery hemodynamics." *Journal of Advanced Research in Applied Sciences and Engineering Technology* 26, no. 2 (2022): 29-40. <https://doi.org/10.37934/araset.26.2.2940>
- [34] Niknahad, Ali. "Numerical study and comparison of turbulent parameters of simple, triangular, and circular vortex generators equipped airfoil model." *Journal of Advanced Research in Numerical Heat Transfer* 8, no. 1 (2022): 1-18.
- [35] Shiono, Mitsuhiro, Katsuyuki Suzuki, and Seiji Kiho. "An experimental study of the characteristics of a Darrieus turbine for tidal power generation." *Electrical Engineering in Japan* 132, no. 3 (2000): 38-47. [https://doi.org/10.1002/1520-6416\(200008\)132:3<38::AID-EEJ6>3.0.CO;2-E](https://doi.org/10.1002/1520-6416(200008)132:3<38::AID-EEJ6>3.0.CO;2-E)
- [36] SÁNCHEZ, Alejandro RUIZ, Angie GUEVARA MUÑOZ, Jorge Andrés Sierra Del Rio, and Jose Alejandro POSADA MONTOYA. "Numerical comparison of two runners for gravitational vortex turbine." *Engineering Transactions* 69, no. 1 (2021): 3-17.